Supporting Information

Materials

Sodium hyaluronate (M.W. = 2.344 x 10^5 Da), purchased from Lifecore Biomedical (Chaska, MN), was used after being dialyzed against distilled water followed by lyophilization. Ethylenediamine, 1-ethyl-3-(3-dimethylaminopropyl) carbodiimide (EDC), N-hydroxysuccinimide (NHS), 5β-cholanic acid, 1-hydroxybenzotriazole (HOBt), fluoresceinamine (FA), and hyaluronidase (Hyal) from bovine testes were purchased from Sigma-Aldrich (St. Louis, MO). The NIR dye, Cy5.5 NHS ester (Cy5.5), was purchased from GE Healthcare (Piscataway, NJ). DOTA-NH_2 was purchased from Macrocyclics (Dallas, TX). Nanocarbons including short single walled carbon nanotubes with an outer diameter of 1-2 nm and a quoted purity of > 90 wt% and short multi-walled carbon nanotubes with an outer diameter > 50 nm and a stated purity of > 95 wt% were purchased from CheapTubes Inc. (Brattleboro, VT). Fullerenes, sublimed with a purity of 99.9%, were purchased from Aldrich. All nanocarbons were directly used, without additional processing. The water, used for synthesis and characterization, was purified by distillation, deionization, and reverse osmosis (Milli-Q Plus). All other chemicals were analytical grade and used without further purification.

SCC7 (squamous cell carcinoma) and 3T3 (fibroblast) cell lines were obtained from the American Type Culture Collection (Manassas, VA). SCC7 cells were kept at 37 °C and 5% CO_2 in RPMI-1640 media (Cellgro, Manassas, VA) supplemented with 10% fetal bovine serum (Invitrogen, Grand Island, NY); while 3T3 cells were incubated in the same conditions in DMEM media (Cellgro) supplemented with 10% fetal bovine serum (Invitrogen).

Synthesis and Characterization of HAC

The synthesis of HAC was previously reported.[1] Briefly, a hydrophobic bile acid, 5β-cholanic acid was conjugated onto water soluble HA polymer via amide formation. First, 5β-cholanic acid was converted to aminoethyl 5β-cholanoamide (EtCA) and reacted via EDC and NHS chemistry with the carboxylic acids of hyaluronic acid. The EtCA content in the conjugate was determined using ^{1}H NMR (UnityPlus 300, Varian, CA), for which the sample was prepared by dissolving in D_2O/CD_3OD (1:1, v/v). To visualize cellular uptake of HAC-coated SWCNTs (HA-NT), HAC was labeled with fluorescein amine

(HAC_{FA}) as previously described.[2] About 130 FA molecules were conjugated to each HAC chain. For *in vivo* photoacoustic monitoring and near infrared fluorescence (NIRF) imaging of HA-NT, Cy5.5 was labeled onto HAC ($HAC_{Cy5.5}$). Cy5.5-hydrazide was chemically conjugated onto HAC through amide formation in the presence of EDC and HOBt, as we previously reported.[3] About 6 Cy5.5 molecules were conjugated to each HAC chain. The amount of FA and Cy5.5 conjugated onto HAC was calculated using an absorbance v.s. concentration curve, obtained by UV/Vis spectrophotometery at 675 nm and 450 nm, respectively.

Surfactant Coating on Nanocarbons

To disperse nanocarbons in HAC solution, a 2:1 weight ratio of HAC to nanocarbons was dispersed in distilled water (DW). For example, 2.5 mg of short SWCNTs were dispersed in 5 mg of HAC in 5 mL DW in a 15 mL Falcon tube. The solutions were then dispersed via probe sonication using a VCX-750 ultrasonic processor (Sonics & Materials, Newtown, CT). The ultrasonic probe (6 mm microtip extension, Sonics & Materials) was immersed into the mixture with a volume ranging from 5 - 10 mL. The probe was driven at 60% of the instrument's maximum amplitude for 60 min at ~ 20 kHz with a 10 sec on / 1 sec off pulse sequence. To avoid heating, the solution was immersed in an ice-bath during sonication. For experiments using HAC-coated SWCNTs (HA-NT), further purification was performed. After sonication, the solution was divided into 500 μL aliquots and purified by a disposable PD-10 desalting column (GE Healthcare).

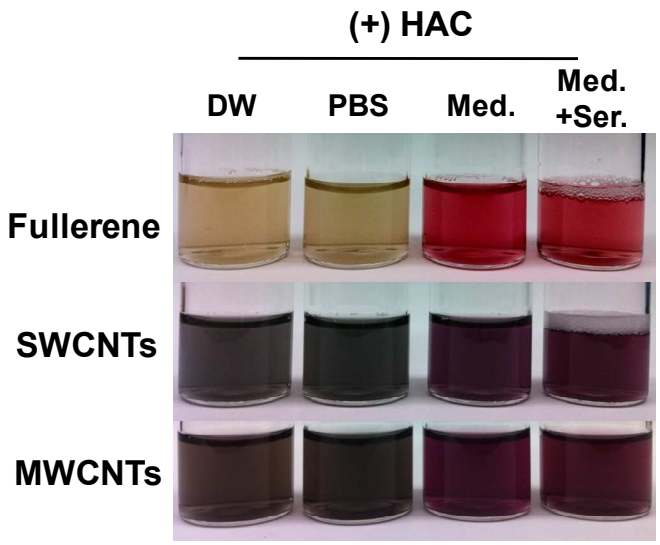

Figure S1. Photographs of nanocarbons from Fig. 1C after 3 months.

Atomic Force Microscope analysis of HA-NTs

After being diluted in DW at 100 µg/mL, HA-NTs were examined under a PicoForce Multimode AFM (Bruker, CA) consisting of a Nanoscope® V controller, a type E scanner head, and a sharpened TESP-SS (Bruker, CA), OMCL (Bruker, CA).

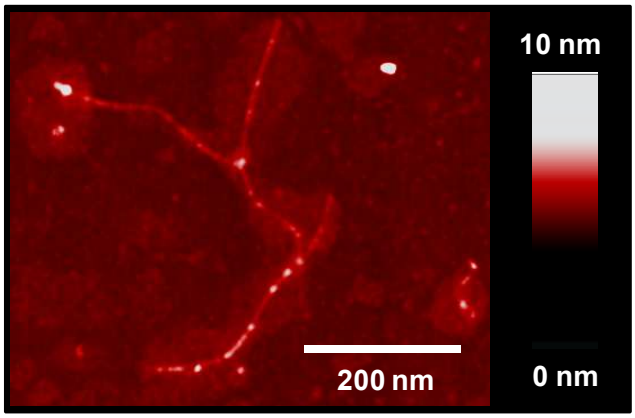

Figure S2. AFM phase image of HA-NTs dispersed in DW.

Raman Readings

Raman characterization was used for the analysis of HA-NTs using the CNT Raman signature G band peak for concentration verification. Raman spectra were recorded on an iRaman 785 (B&W Tek, Inc, DE) spectrometer with a BCF100A cuvette holder. Known concentrations of HA-NTs were measured in cuvettes with a power output of 35 mW. The excitation source was an argon ion laser, 785 nm.

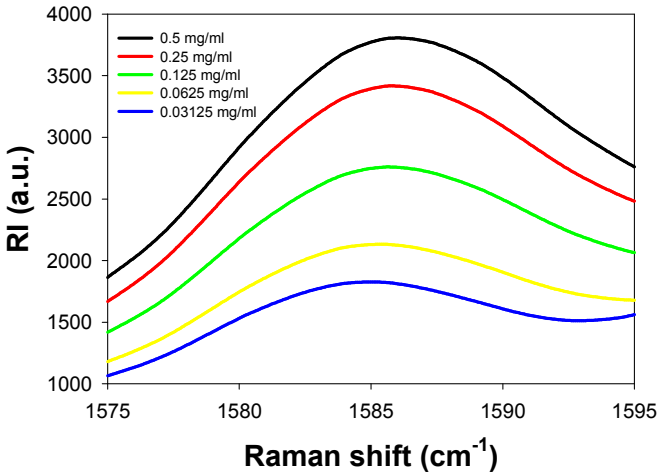

Figure S3. Raman G-band of HA-NTs at a concentration range from 0.0325 – 0.5 mg/mL.

Absorbance Readings

To estimate the concentration of SWCNTs in the solution, a calibration curve by UV-Vis absorbance was performed on samples with known concentrations. Absorbance was measured by a Genesys 10S UV-Vis Spectrophotometer (Thermo Scientific, Waltham, MA). The absorbance at 808 nm was used as a marker for the concentration of SWCNTs. After sonication of a known concentration of SWCNTs, absorbance was collected and the value was standardized to the SWCNT concentration. Absorbances of HA_{FA}-NT and $HA_{Cy5.5}$-NT were collected using the Genesys 10S system and normalized using Prism Version 4 for Windows (Graphpad, La Jolla, CA).

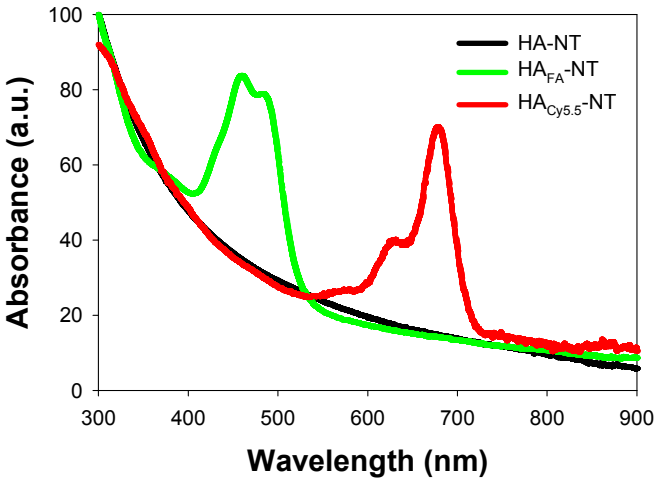

Figure S4. Normalized UV/Vis absorbance spectra of HA-NTs, HA_{FA}-NTs, and $HA_{Cy5.5}$-NTs

Fluorescence Measurements

Fluorescence intensity was monitored with an F-7000 fluorescence spectrophotometer (Hitachi, Tokyo, Japan). Fluorescence was collected for $HAC_{FA\ or\ Cy5.5}$ and $HA_{FA\ or\ Cy5.5}$-NT at the same concentrations $HAC_{FA\ or\ Cy5.5}$ (3.3 – 213 nM). For HAC_{FA}, the excitation wavelength was set at 490 nm and emission was collected at 525 nm. For $HAC_{Cy5.5}$, the excitation wavelength was set at 675 nm and emission was recorded at 695 nm. To show the quenching potential of $HA_{FA\ or\ Cy5.5}$-NT, the fluorescence was recorded as emission fluorescence value over the initial emission fluorescence value (F/F_0) at 3.3 nM. Therefore, the y-axis value represents the amount of fold the fluorescence emission increased as the concentration of $HAC_{FA\ or\ Cy5.5}$ increased. The fluorescence activation of HA-NTs after hyaluronic acid degradation was observed by incubating the HA_{FA}-NT (HA_{FA}: 2.1 μM) in DI with Hyal (400 unit/mL) in PBS with pH 4.5 at specified time points. Fluorescence spectra for HA_{FA}-NT and $HA_{Cy5.5}$-NT were excited at 490

nm and 675 nm, respectively and collected from 500 to 600 nm and 680 to 750 nm, respectively, at a scan speed of 240 nm/min. Fluorescence spectra were recorded as the direct output from the spectrophotometer with a PMT voltage of 950V, using the same Hitachi fluorescence spectrophotometer. The effect of enzyme concentration (12.25 - 400 unit/mL) and time on fluorescence activation of dye HA_{FA}-NT was monitored using the optical imaging system, a Maestro all-optical imaging system (Caliper Life Sciences, Hopkinton, MA) in a clear 96-well plate.

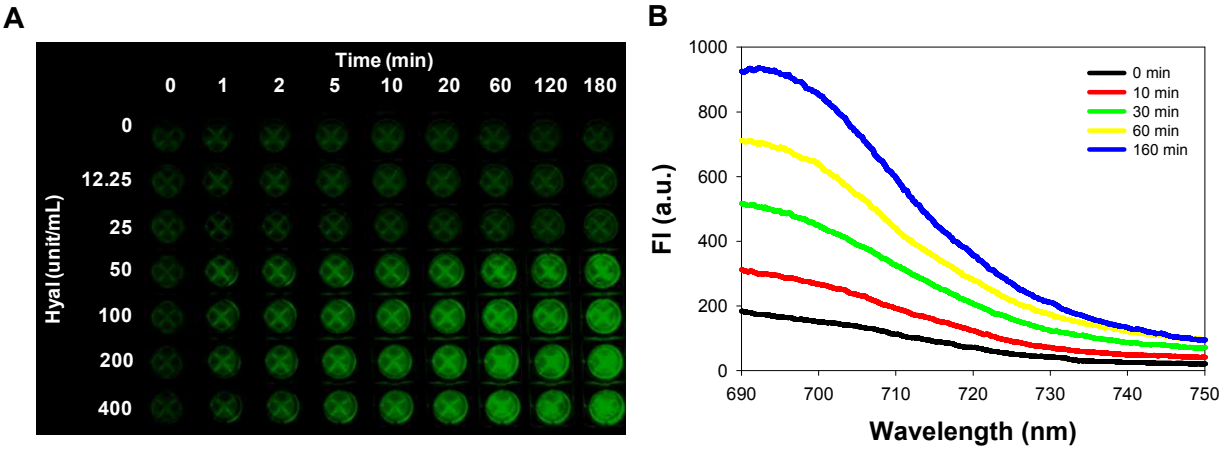

Figure S5. (A) Fluorescence imaging using an optical imaging system of HA_{FA}-NTs activated with hyaluronidase over different concentrations of enzyme and time. (B) $HA_{Cy5.5}$-NTs fluorescence (ex: 675 nm) after 400 units of hyaluronidase was added to 50 µg/mL of $HA_{Cy5.5}$-NTs over time.

In vitro Cellular Uptake of HACA-SWCNTs

Confocal Imaging of HA_{FA}-NT. SCC7 and 3T3 cells were plated at least 24 h before incubation with HA_{FA}-NT in LabTek II coverglass (Nalge Nunc International, Rochester, NY) at a density of 5 x 10^4 cells/mL and grown to 60 - 80% confluence. The cells were incubated with 50 µg/mL of HA_{FA}-NT in serum free media for 30 or 180 min. For competitive inhibition studies, the medium of SCC7 cells was replaced with 2 mL of serum-free culture medium containing HA (10 mg/mL) and 50 µg/mL of HA_{FA}-NT and incubated for 180 min. After incubation, the cells were thoroughly washed twice with PBS and examined by an inverted Zeiss LSM 700 confocal microscope (Carl Zeiss MicroImaging GmbH, Germany). Imaging was carried out at 37 °C in 5% CO_2. Images were acquired and processed with the Zeiss Zen 2009 image software. The fluorescence micrographs shown are representative of at least three

independent experiments. Individual cell profiles from confocal microscopy images were processed for fluorescence intensity using Image J (NIH, Bethesda, MD).

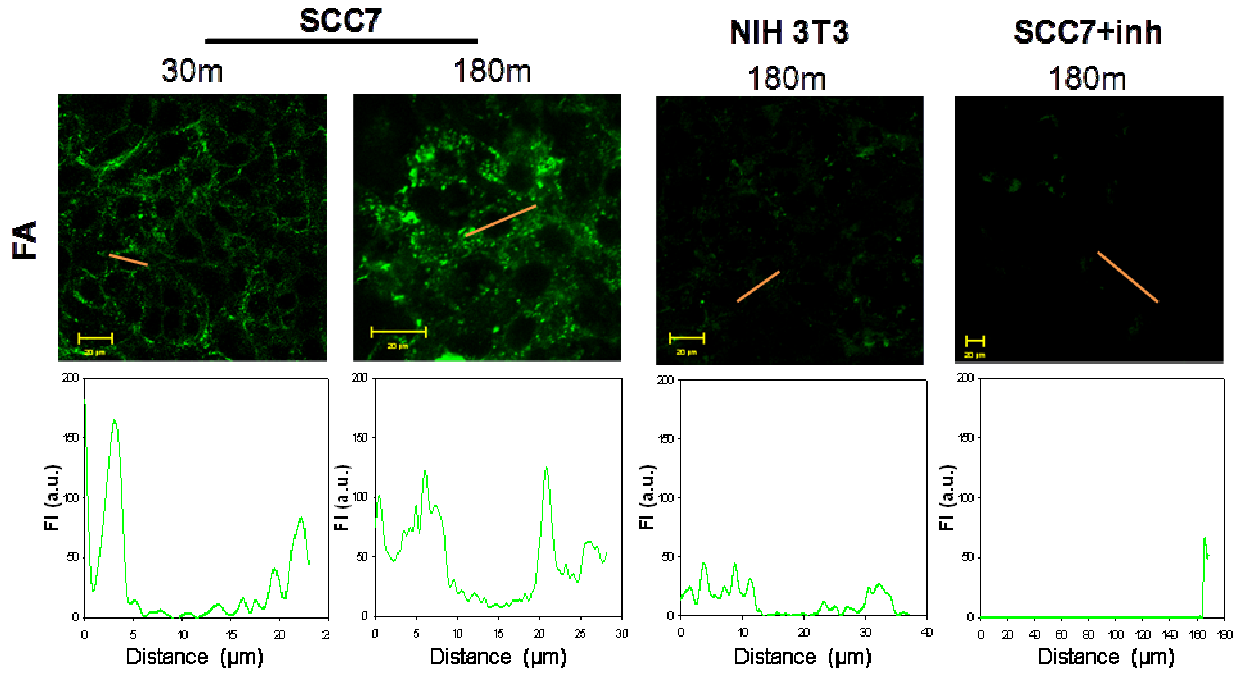

Figure S6. Confocal fluorescence images and intensity profiles of CD44 positive SCC7 cells and CD44 negative 3T3 cells treated with HA_{FA}-NTs for 30 and 180 min. SCC7 were inhibited by excess HA (SCC7 + inh).

Fluorescence Activated Cell Sorting. FACS was collected by Accuir C6 flow cytometer using CFlow Plus software (BD, Ann Arbor, MI) and used to determine CD44 labeling and intracellular FA fluorescence. FACS data was analyzed using FlowJo version 7.6.5 (FlowJo, Ashland, OR). All data was analyzed using 5,000 cells. For CD44 labeling, rat anti-mouse CD44 primary antibody diluent (1:50) was subsequently applied to SCC7 and 3T3 cells, and the incubation was left at 2 - 8 °C for 30 min. After rinsing twice with Flow Cytometry Staining Buffer, a biotinylated anti-rat IgG secondary antibody solution (1:50) was applied, and the mixture was incubated at 2 - 8 °C for 30 min. For HA_{FA}-NT uptake analysis, SCC7 and 3T3 cells were treated with 50 μg/mL of HA_{FA}-NT for 0, 30, 90 and 180 min and collected by Accuir C6 flow cytometer.

Confocal Raman Mapping and Z-profiling. Raman spectra were collected with 9-18 cm^{-1} resolution using a confocal Raman microscope (Senterra, Bruker Optics, Billerica, MA) equipped with a 40 X/0.95 NA objective, 50 μm pinhole, 785 nm laser (35 mW at sample, 90-3200 cm^{-1} spectral range), 532 nm laser (14 mW, 40-4500 cm^{-1}) and transmission/fluorescence microscopic system.

For Raman mapping, SCC7 and 3T3 cells were incubated in 35 mm glass bottom petri dishes (MatTek, Ashland, MA). After 50% confluency was reached, cells were treated with 50 μg/mL of HA_{FA}-NT for 3 hours, washed, and then fixed using Z-fix (Anatech, Battle Creek, MI). To monitor the morphology of cells, SCC7 and 3T3 cells treated with HA_{FA}-NTs were washed three times with HEPES buffer followed by staining actin filaments with rhodamine-phalloidin (Invitrogen). Pseudo-phase contrast and FA fluorescence images of the cells were collected using the Raman system and overlayed by ImageJ. The 785 nm-laser was focused to 2 μm diameter spots at perinuclear area and cytoplasm, and Raman-scattered light was collected from ~2x2x7 μm focal volume for 10 s per point.

For Raman z-profiling, SCC7 cells plated on glass slides were treated with 100 μg/mL of HA-NT for 3 h, removed from glass by trypsin and fixed in suspension with 4% paraformaldehyde. The fixed cells were then drop-cast between 1 mm and 0.16 mm quartz slides. Raman mapping with the 532 nm-laser (~2x2x5 μm focal volume) was first used to locate a large G-band signal. Then, the 532 nm-laser was focused at such locations, and Raman spectra were collected along z-step sizes of 1-3 μm for 10 s per step. Water and slide contributions were subtracted prior to analysis of the resulting spectra.

Small Animal Imaging

^{64}Cu-labeling. For *in vivo* PET imaging, DOTA-NH_2 was conjugated onto HAC through amide formation in the presence of EDC and HOBt. SWCNTs were dispersed with DOTA-labeled HAC (HAC_{DOTA}) as we described above, which resulted in clear dispersion of SWCNTs wrapped with HAC_{DOTA} (HA_{DOTA}-NTs) in DW. In addition, HA_{DOTA}-NTs were labeled with ^{64}Cu. $^{64}CuCl_2$ was converted to $Cu(OAc)_2$ by adding 0.5 mL of 0.4 M ammonium acetate (NH_4Ac, pH 5.5) to 20 μL $^{64}CuCl_2$. $Cu(OAc)_2$ (1 mCi) was added into a solution of HA_{DOTA}-NTs and incubated for 1 h with constant agitation. The labeled particles were purified with a PD-10 column to remove unreacted ^{64}Cu molecules. The labeled efficiency was calculated based on the radiation dosimeter readings before and after purification. The radio-labeling yield was 70 to 80%.

In vivo PET Imaging of HA-NT Tumor Uptake. Tumor-bearing mice were prepared by subcutaneously injecting a suspension of 1×10^6 SCC7 cells in physiological saline (100 μL) into the front flank of athymic nude mice (seven weeks old, 20 – 25 g). When the tumor size reached 100 mm^3, 100 μL of 100 - 200 μCi ^{64}Cu-labeled HA-NT was intravenously injected into the SCC7 tumor-bearing mice. PET scans were performed with a microPET R4 rodent scanner (Siemens Medical Solutions) at pre-determined time points. For each scan, 3-dimensional ROIs were drawn over the tumor and organs on decay-corrected whole-body coronal images. The average radioactivity concentration was obtained from the mean pixel values within the ROI volume, and was converted to counts per milliliter per minute by using a predetermined conversion factor.[6, 7] Given a tissue density of 1 g/mL, the counts per milliliter per minute were converted to counts per gram per minute, and the values were divided by the injected dose to obtain the imaging-ROI-derived percentage injected dose per gram (% ID/g). At the end of the 48 h scan, the mice were sacrificed, and the tumors as well as the major organs were collected and subjected to an *ex vivo* PET scan.

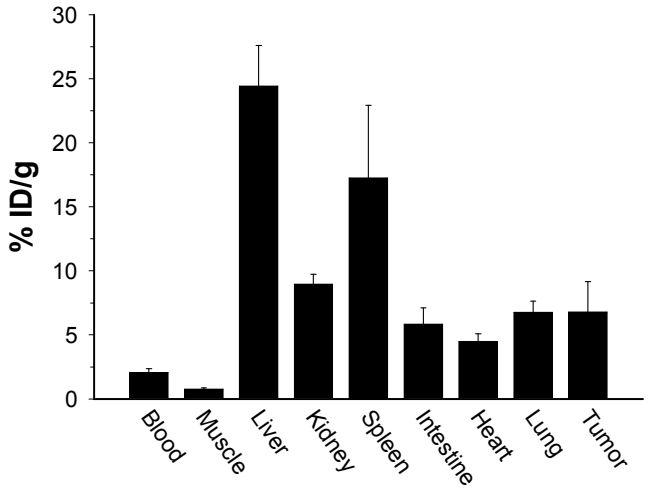

Figure S7. Injected dose per gram of PET data distributed over major organs after 48 hours. Error bars represent S.D., n=3 mice.

Photoacoustic Imaging. Tumor-bearing mice were prepared by subcutaneously injecting a suspension of 1×10^6 SCC7 cells in physiological saline (100 μL) into the front flank and hind limb of athymic nude mice (seven weeks old, 20 – 25 g). After fourteen days of subcutaneous inoculation, $HA_{Cy5.5}$-NTs were injected into the tail vein of the tumor-bearing mice at a dose of 5 mg/kg SWCNT. Photoacoustic

imaging (Vevo 2100, VisualSonics, New York, NY) was performed on the hind limb tumors of three mice after 150 μL of $HA_{Cy5.5}$-NTs were injected in the tail vein. Ultrasound and photoacoustic images of the tumor were taken at pre-injection and at 2 h and 20 h post-injection. All photoacoustic intensities were normalized for laser energy. The nanostepper feature of the system was used to measure photoacoustic intensities across 680 - 970 nm wavelengths. Images and intensities at 680 nm were used for analysis.

In vivo/Ex vivo NIRF Imaging. After intravenous injection of $HA_{Cy5.5}$-NTs at a dose of 5 mg/kg SWCNT, biodistribution and tumor accumulation profiles were monitored on the front flank tumors of three mice by using a Maestro all-optical imaging system at predetermined time points (24, 48, 72 and 96 h). For all imaging procedures, mice were anesthetized with 3% to 4% isoflurane using a nose-cone manifold and restrained on the imaging stage. Major organs and tumors were dissected from SCC7 tumor-bearing mice at 96 h after intravenous injection of $HA_{Cy5.5}$-NTs (5 mg/kg). NIR fluorescence images of dissected organs and tumors were obtained with the Maestro all-optical imaging system. The tissue distribution of $HA_{Cy5.5}$-NTs was quantified by measuring NIR fluorescence intensity at the ROI. All values are expressed as means ± S.D. for groups of three animals.

Ex vivo Cryo-TEM Imaging. To observe tissue distribution of HA-NTs in tumor, the dissected tumors were fixed in a 4% formaldehyde solution for 10 min at room temperature, and embedded in OCT medium (Miles Inc, Elkhart, IN, USA). The tumors were frozen and sections (10 mm in thickness) were cut on a cryostat. Tissue distribution of HA-NTs was observed using a Tecnai TF30 electron microscope (FEI Company) equipped with a GIF Tridiem imaging filter (Gatan Inc.) and operated at an accelerating voltage of 300 kV.

Statistical Analysis

The statistical significance of differences among the groups tested was determined using one-way ANOVA. A p-value less than 0.05 was considered significant and is specified in the figures with an asterisk.

1. Choi, K. Y.; Min, K. H.; Na, J. H.; Choi, K.; Kim, K.; Park, J. H.; Kwon, I. C.; Jeong, S. Y. *J Mater Chem* **2009,** 19, (24), 4102-4107.

2. de Belder, A. N.; Wik, K. O. *Carbohydr Res* **1975,** 44, (2), 251-7.
3. Choi, K. Y.; Chung, H.; Min, K. H.; Yoon, H. Y.; Kim, K.; Park, J. H.; Kwon, I. C.; Jeong, S. Y. *Biomaterials* **2010,** 31, (1), 106-14.
4. Ali-Boucetta, H.; Al-Jamal, K. T.; Kostarelos, K., Cytotoxic Assessment of Carbon Nanotube Interaction with Cell Cultures. In 2011; Vol. 726, pp 299-312.
5. Wörle-Knirsch, J. M.; Pulskamp, K.; Krug, H. F. *Nano Letters* **2006,** 6, (6), 1261-1268.
6. Cai, W.; Wu, Y.; Chen, K.; Cao, Q.; Tice, D. A.; Chen, X. *Cancer Res* **2006,** 66, (19), 9673-81.
7. Cai, W.; Chen, K.; He, L.; Cao, Q.; Koong, A.; Chen, X. *Eur J Nucl Med Mol Imaging* **2007,** 34, (6), 850-8.